The origin of N_2-H_2-CH_4-rich natural gas seepages in ophiolitic context: A major and noble gases study of fluid seepages in New Caledonia

Eric Deville *, Alain Prinzhofer [1]

IFPEN, 1-4, av. de Bois-Préau, 92 852 Rueil-Malmaison Cedex, France

ARTICLE INFO

ABSTRACT

The study of natural gas seepages in New Caledonia has shown the occurrence of two gas families, one is N_2-H_2-CH_4-rich, the other is N_2-rich. The N_2-H_2-CH_4-rich gases are bubbling in hyperalkaline springs (OH^--rich) known in the peridotite massif of the southern part of the island. This family of gas shows contents of N_2 between 50 and 62%, H_2 between 26 and 36%, and CH_4 between 11 and 16%. $\delta^{13}C$ values of methane are ranging from -39 to $-32‰$. We interpret the origin of H_2 as a product of fluid-rock interaction between basic-ultrabasic rocks and water with oxidation of Fe^{2+} and reduction of underground water in the fracture system of the peridotites nappe. Methane is interpreted as the result of a reduction of dissolved inorganic and/or organic carbon in subsurface aquifers. The second family of gas emissions was found in thermal springs in the sedimentary units located structurally below the peridotites nappe. The gas is composed mostly of N_2 (between 97 and 98%) associated with relatively high concentration of He. Both gas families show notably high N_2 vs fossil noble gas contents (^{36}Ar, ^{20}Ne, ^{84}Kr) suggesting that N_2 is not directly issued from gas dissolved in aquifers equilibrated with atmosphere but most likely finds its origin in a deep source, probably within metamorphic sediments which are tectonically buried below the ophiolitic nappe. We interpret the N_2-H_2-CH_4-rich family of gas as a result of a mixing between two end-members, (1) a H_2-CH_4-rich pole issued from the weathering of peridotite rocks and (2) a N_2-rich pole which would be issued from the metamorphosed sediments buried below the ophiolitic units. An unusual inverse correlation between the atmospheric noble gas isotopes ^{20}Ne and ^{36}Ar is interpreted as the result of a degassing of a relatively shallow confined aquifer related to a bubble flow from depth.

© 2016 Elsevier B.V. All rights reserved.

1. Introduction

Natural molecular hydrogen associated with methane and nitrogen has been reported several times in ophiolitic context either bubbling or simply dissolved in hyperalkaline spring water issued from serpentinized peridotites massifs, notably in Oman (Neal and Stanger, 1983; Sano et al., 1993), in the Philippine Archipelago (Abrajano et al., 1988, 1990), the Sakalin and Koryak Plateau in Russia (Smith et al., 2005), Milford Sound in New Zealand (Wood, 1970), Canada (Szponar et al., 2013), or Japan (Suda et al., 2014), and others. Also, as it is the case of the gas seeping out from ophiolitic rocks, H_2-rich fluids associated with N_2 and CH_4 contents are well-known in deep-water hydrothermal seepages of different areas of mid-oceanic ridges (Welhan and Craig, 1979; Kelley and Früh-Green, 1999; Charlou et al., 2002; Kelley et al., 2005; Proskurowski et al., 2008, and others). This type of gas

seepage has always been interpreted as the result of ultrabasic rock alteration during serpentinization processes which are indeed able to generate molecular hydrogen and abiotic methane (meaning methane whose generation is not linked with organic matter thermal cracking but involves molecular hydrogen reducing any source of carbon). This interpretation well explains the nature of gas seepages discovered in ophiolitic context showing high contents in H_2 and CH_4 with high values of $\delta^{13}C$ ($>-20‰$), notably gas samples studied in Oman (Vacquand, 2011), the Zambales ophiolite in Luzon, in the Philippines (Abrajano et al., 1988, 1990) and in Southern Turkey (Hosgormez et al., 2008). But, so far, no publication has really attempted to explain the constant association of molecular nitrogen with these H_2-CH_4-bearing gases. One possibility is that N_2 is simply of atmospheric origin and passively taken from the aquifers or the sea water during hydrothermalism dynamics and/or bubbling processes of the H_2-CH_4-bearing gas. However this interpretation is more questionable when N_2 becomes the dominant phase in the gas seepages. We present in this paper a study of the gas composition of seepages located inside and in the vicinity of the New Caledonian ophiolite for which we tried to understand better the origin of N_2-H_2-CH_4-rich gas seepages in the ophiolitic rocks and N_2-rich gas seepages structurally below the ophiolitic rocks. This work is based on analyses on the major gases and noble gases.

---

* Corresponding author.
  E-mail address: eric.deville@ifpen.fr (E. Deville).
[1] Present address: GEO4U, Praia de Botafogo 501, 22250-040 Rio de Janeiro, Brazil.

2. Geological setting of the gas seepages

The geology of New Caledonia is characterized by large outcrops of ophiolitic rocks (mainly peridotites; i.e. Fe-Mg silicates) that make one of the largest onshore massif of ultrabasic rocks preserved on Earth (Fig. 1A). The ophiolitic rocks of New Caledonia correspond to outcrops of the south-western edge of the lithospheric mantle forming the basement of the Loyalty oceanic basin (Prinzhofer et al., 1980; Cluzel et al., 2001). They are notably well exposed in the southern part of the island and they also form a series of klippes (chief mountains), in the north-western part of the island (Fig. 1A). The peridotites nappe was emplaced during Eocene times over formations of continental affinity (Paris, 1981; Cluzel et al., 2001; Fig. 1B) including (1) a basement of arc-derived formations of Pre-Cretaceous age which are overlain by basalts and formations of the Central Range that include sandstones, silt-stones, grauwaches, claystones with coal of Cretaceous age and Tertiary carbonate turbidites and volcaniclastic deposits (Paris, 1981), and (2) a tectonic unit of oceanic basalts of Upper Cretaceous to Eocene age, with back-arc or fore-arc affinities which underlies the peridotites nappe (Paris, 1981; Cluzel et al., 2001). The gas seepages studied here were found within the peridotite nappe and also within grauwaches

formations located structurally just under the nappe of the peridotites, in the area of La Crouen (Fig. 1A).

3. The gas-bearing springs

In the whole New Caledonia Territory, gas seepages were found in different contexts, either in the onshore, in the foreshore and in the near offshore (photo A in supplementary material). These gas seepages were sampled in two different types of springs. The first type corresponds to hyperalkaline thermal springs (with pH ranging from 10.5 to 10.9; Table 1). These hyperalkaline springs are located in the Prony area (Fig. 1). Their waters have already been studied by Barnes et al. (1978); Cox et al. (1982); Launay and Fontes (1985) and Monnin et al. (2014) in the Carenage Bay, the Kaori Bay, and offshore in the Roc Ai-guille (also called needle of Prony), in all cases within the ophiolitic nappe of New Caledonia. The water is characterized mostly by the oc-currence of Ca^{2+} (20–22 mg/l), Na^{2+} (11–14 mg/l), a little K^+ (1–1.5 mg/l), Cl^- (10–11 mg/l), SiO_2 (3 mg/l), OH^- (21–24 mg/l) and no HCO_3^- or CO_3^{2-}. Therefore the OH^- concentration is only responsible for the alkalinity of this thermal water. The springs in the foreshore (Carénage and Kaoris) and the offshore (Roc Aiguille) are associated
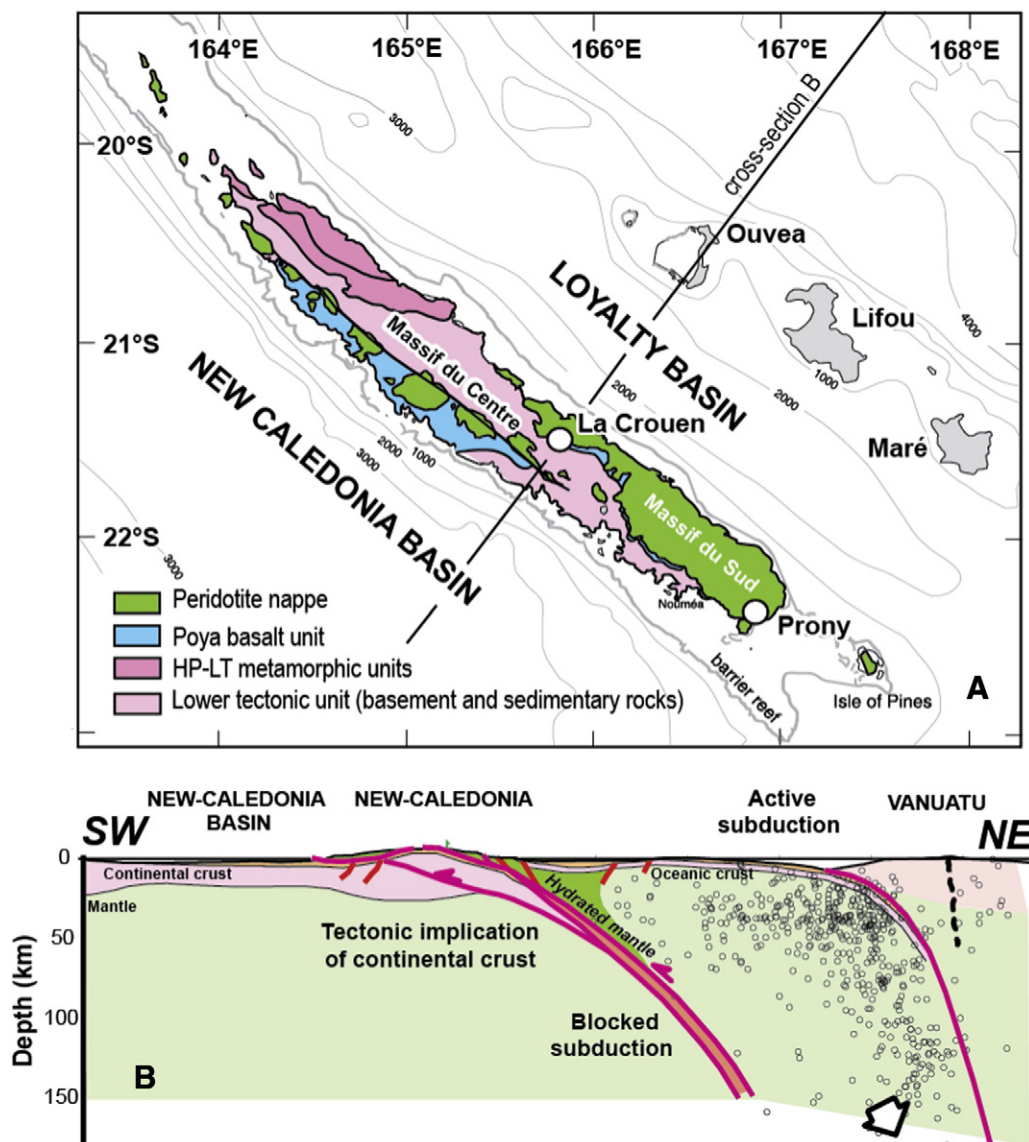

Fig. 1. Structural sketch-map (A) and simplified geological cross-section (B) of New Caledonia. Circles in B correspond to earthquake hypocenters. They well illustrate that the subduction north of New Caledonia is inactive today and that the Vanuatu subduction zone is active.

Table 1
Temperature, pH, Eh and electric conductivity of the studied springs.

Site	X	Y	T°C	pH	Eh	Conductivity
	WGS84		(°C)		(mV)	(mS/cm)
Carénage 1	166° 50′ 27.4″ E	22° 18′ 17.3″ S	40.0	10.84	−285	0.54
Carénage 2	166° 50′ 27.6″ E	22° 18′ 17.3″ S	40.1	10.52	−800	0.483
Kaoris 1	166° 51′ 42.5″ E	22° 17′ 57.9″ S	31.6	10.86	−480	0.41
Kaoris 2	166° 51′ 42.5″ E	22° 17′ 57.8″ S	30.4	10.64	−230	1.185
Kaoris 3	166° 51′ 42.4″ E	22° 17′ 57.9″ S	30.5	10.58	−285	0.414
La Crouen 1	165° 53′ 20.7″ E	21° 32′ 06.8″ S	41.5	9.16	−226	0.313
La Crouen 2	165° 53′ 20.6″ E	21° 32′ 06.7″ S	41.2	9.2	−230	0.314
Roc Aiguille 1	166° 50′ 6″ E	22° 19′ 44″ S	23.5	9.9	−180	8.03
Roc Aiguille 2	166° 50′ 6″ E	22° 19′ 44″ S	23.5	10.03	−210	8.36

with a precipitation of primary brucite ($Mg(OH)_2$; photo B in supplementary material) and Ca-carbonates (calcite and aragonite), the magnesium of the brucite being provided by the sea water (Launay and Fontes, 1985). The observed fluid flows in the Prony area were consistent with the values mentioned in Launay and Fontes (1985); i.e. 6 m^3/day of gas and 15 m^3/day of water for the Carénage springs and 4 m^3/day of gas and 10 m^3/day of water for the Kaoris springs. During our visit, the temperature of the water was ranging between 40.0 and 40.1 °C in the Carénage springs and between 30.4 and 31.6 °C in the Kaoris springs. We noticed extremely reducing conditions on these springs with measured oxydo-reduction potential (Eh) down to −800 mV in one of the vent of the Carénage (Fig. 2A). This low Eh value corresponds to the high temperature of spring water in the Prony area (40.1 °C). The electric conductivity being between 0.3 and 1.2 mS/cm reflects the moderate salinity of the water. The water characteristics of the Roc Aiguille seeps is more difficult to define precisely because the seepage occurs under the sea, so there is a mixing with sea water, but it also corresponds to alkaline water (measured pH between 9.90 and 10.03) and reducing water (measured Eh between −210 and −180 mV; Table 1).

The second type of spring corresponds to a hydrothermal site with moderately alkaline water (pH between 9.16 and 9.2) with also low Eh values (−226 to −230 mV). These springs are located in the area of La Crouen and they have been already mentioned by Cox et al. (1982). The nature of the water is different from the springs of the area of Prony with Ca^{2+} (1 mg/l), Na^{2+} (55.4 mg/l), K$^+$ (1.9 mg/l), Mg^{2+} (0.2 mg/l), Cl$^-$ (12.2 mg/l), SiO$_2$ (60 mg/l) and HCO$_3^-$ (15 mg/

l)(Cox et al., 1982). These thermal springs are located in sediments situated structurally under the ophiolitic nappe in the central chain of New Caledonia. During our visit, the temperature of these springs was ranging between 41.2 and 41.5 °C (Fig. 2B).

4. Methodology

Free gas phases were present in the springs of La Crouen and in the Prony area. In the Roc Aiguille no free-gas phase was emitted but water samples were degassing after sampling and this gas was also analyzed. For the analysis of the major gases and the carbon isotopic ratios, the gas was collected with a funnel in glass containers (vacutainers©) prepared under secondary vacuum. Gas samples devoted to noble gases study were collected with a funnel in evacuated stainless steel containers prepared under secondary vacuum. The major compound concentrations (CH_4, C_2H_6, C_3H_8, C_4H_{10}, CO_2, N_2, H_2, O_2, and H_2S) were determined by chromatography in gas phase using a Varian chromatograph (GC) equipped with three columns and with two detectors (flame ionization detector [FID] and thermal conductivity detector [TCD]). Carbon isotopic ratios of CH_4 were determined with a Thermo-Finnigan GC-C-IRMS (gas chromatography-mass spectrometer coupling). The noble gases elemental compositions of ^{4}He, ^{20}Ne, ^{36}Ar and ^{84}Kr and the isotopic ratios ^{40}Ar/^{36}Ar were determined by quadrupole mass spectrometry (QMA/QME200) after treatment of the gas sample through an ultra-high vacuum preparation line. Helium isotopic ratios were determined by the means of a high-resolution magnetic sector mass spectrometer Micromass VG5400.
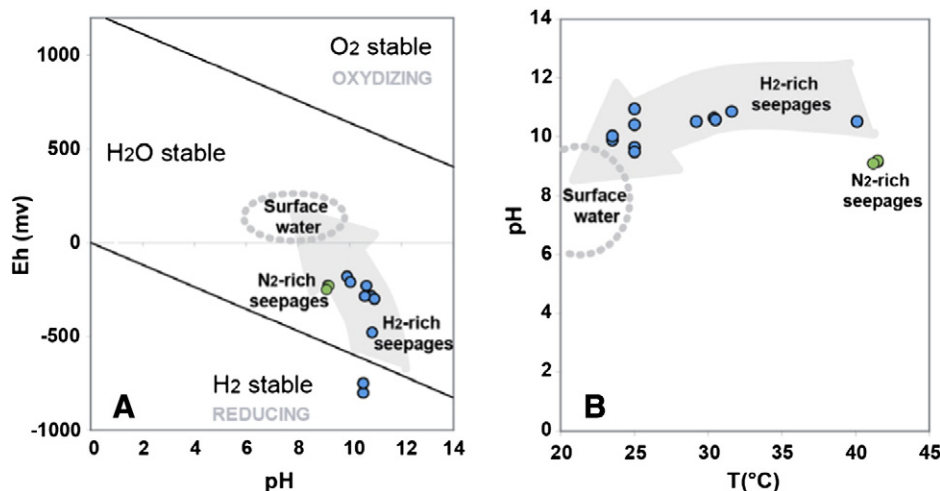

Fig. 2. Diagrams pH-Eh (A) and Temperature-pH (B) showing some of the major physico-chemical parameters of the water where the gas sample were taken.

5. Results

Among the collected gas samples, we identified two types of gaseous emanations (1) N_2-H_2-CH_4-rich gas seepages and (2) N_2-rich gas seepages (Fig. 3). The occurrence of N_2-H_2-CH_4-rich gas seeping in several springs of New Caledonia was already mentioned in Deville et al. (2010) and this was recently confirmed in Monnin et al. (2014). The N_2-H_2-CH_4-rich seepages which have been sampled in this study are located inside the peridotites nappe of New Caledonia in the Prony area, in the southern part of the island (Massif du Sud) in the hyperalkaline springs of the Carénage and Kaoris bays. Note that the pH of the water is slightly lower (between 10.58 and 10.86) and the temperature slightly higher compared to other H_2-bearing springs known in Oman which have pH between 11 and 12 (Neal and Stanger, 1983). The N_2-rich seepages which have been sampled in the thermal springs of La Crouen are located in sedimentary rocks which are structurally located below the peridotite nappe, in the center of the island. The gas is mainly nitrogen (97.22–97.29%) associated with relatively high contents of helium (0.051 to 0.053%; Tables 2 and 3). This gas also contains some methane (2.65 to 2.73%). The degassing phase from the thermal hyperalkaline springs water seeping out offshore from the Roc Aiguille is dominated by N_2 associated with methane and a little hydrogen (Table 2). It was not possible to properly study the noble gas contents of the Roc Aiguille because of too large contamination by the sea water. Note that no C2+ (C_2H_6, C_3H_8, C_4H_{10}, …) were found in any of the gas samples. Noble gas composition was analyzed in the samples of the sites where it was possible to get good sampling (Carénage, Kaoris, La Crouen). The results are presented in Table 3.

6. Discussion

6.1. Hydrogen

In the N_2-H_2-CH_4-rich gas seepages of the Carénage bay and the Kaoris bay, H_2 is thought to be most likely linked with recent alteration processes (serpentinization) of peridotite rocks. High-temperature serpentinization (above 300 °C) is a well-known process but at lower temperatures (50 to 300 °C) serpentinization can occur as well (Moody, 1976). Biological processes can also occur via bacterial anaerobic oxidation of Fe^{2+} using H_2O as an electron acceptor. As it has already been proposed in previous studies on hydrogen-bearing gas seepages associated with high pH waters in ophiolitic context (Barnes et al. 1967; Barnes et al., 1978; Neal and Stanger, 1983; Sano et al., 1993; Cipolli et al., 2004; Hosgormez et al., 2008; Abrajano et al., 2009; Vacquand, 2011), H_2 would result from the interaction between ultrabasic rocks and water flowing at depth in the fracture system, by reduction of water and oxidation of metals (Fe^{2+}, Mn^{2+}, …), Fe^{2+} being by far the most important electron donor in
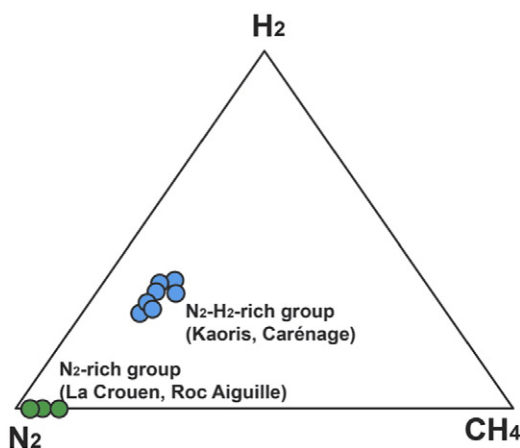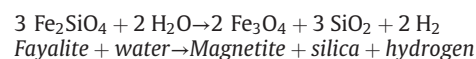
ultrabasic rocks. Fe^{2+} is provided by Fe^{2+}-rich minerals, such as olivine [$(Mg^{2+},Fe^{2+})_2SiO_4$], and it contributes during the serpentinization process to the formation of Fe^{3+}-bearing minerals, such as magnetite. Indeed during olivine dissolution, the iron pole tends to react according to the following equation,

$$3\ Fe_2SiO_4 + 2\ H_2O \rightarrow 2\ Fe_3O_4 + 3\ SiO_2 + 2\ H_2$$
$$Fayalite + water \rightarrow Magnetite + silica + hydrogen$$

It is worth to note that evidences of siliceous diagenetic precipitations associated with the peridotites of New Caledonia are indeed very common (Paris, 1981). On the other side, the magnesian pole reacts as,

$$2\ Mg_2SiO_4 + 3\ H_2O \rightarrow Mg_3Si_2O_5(OH)_4 + Mg^{2+} + 2\ OH^-$$
$$Forsterite + water \rightarrow Serpentine + magnesium + ion\ hydroxyde$$
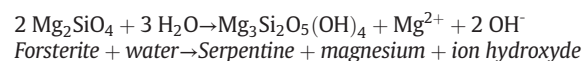
As such, the interaction between peridotite and water during serpentinization is a potential source of H_2 associated with a rise of pH by OH^- production. The richer in iron is the olivine the more H_2 and the less OH^- are produced. During dissolution of olivine, silica produced from hydration of Fe-rich olivine is prone to react with Mg-rich olivine, allowing the following reaction,

$$3\ Mg_2SiO_4 + 4\ H_2O + SiO_2 \rightarrow 2\ Mg_3Si_2O_5(OH)_4$$
$$Forsterite + water + silica \rightarrow Serpentine$$
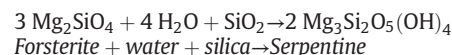
6.2. Methane

About the origin of methane, several processes can be invoked. If dissolved inorganic carbon is available at depth, methane generation can occur by reaction of dissolved inorganic carbon directly with the ultrabasic rocks and water directly in the fracture system (Suda et al., 2014). We can summarize the process according to the following generic reaction,

$$6\ Fe_2SiO_4 + 2\ H_2O + CO_2 \rightarrow 4\ Fe_3O_4 + 6\ SiO_2 + CH_4$$
$$Fayalite + water + carbon\ dioxide \rightarrow Magnetite + silica + methane$$

Table 2
Major gas analyses (% volume) and $\delta^{13}C_1$ values of methane (‰). Note that no C2+ were detected.

Site	H_2	N_2	CH_4	CO_2	$\delta^{13}C_1$
Carénage 1	36.07	50.25	13.68	0	−32.4
Carénage 2	32.40	51.86	15.74	0	
Kaoris 1	26.81	61.90	11.29	0	−38.5
Kaoris 2	32.87	55.29	11.54	0	−34.9
Kaoris 3	29.82	58.92	11.26	0	
La Crouen 1	0	97.22	2.73	0	−39.0
La Crouen 2	0	97.29	2.65	0	−39.5
Roc Aiguille 1	0.095	93.09	5.06	1.75	−12.1
Roc Aiguille 2	0	91.39	8.51	0.1	−16.4

Table 3
Noble gas analyses ^{4}He, ^{20}Ne, ^{36}Ar, ^{84}Kr (ppmv), ^{40}Ar/^{36}Ar, and R/Ra (helium isotopic ratios normalized to the air isotopic Ra = ^{3}He/^{4}He = 1.4 10^{-6}). Global relative uncertainties (at 1σ) for quantification of noble gases with the method used is estimated in the range He: ±10%, Ne: ±20%, Ar: ±5%, Kr: ±10%, and for quantification of the ratio ^{40}Ar/^{36}Ar: ±2%. The global relative uncertainty (1σ) for the R/Ra ratio is in the range ±2%.

Site	^{4}He	^{20}Ne	^{36}Ar	^{84}Kr	^{40}Ar/^{36}Ar	R/Ra
Carénage 1	6.40	13.03	3.37	0.33	308.6	0.43
Carénage 2	3.88	14.97	2.20	0.14	301.2	1
Kaoris 1	3.93	2.48	23.99	0.47	315.2	1.56
Kaoris 2	3.99	5.86	9.97	0.29	301.2	1.73
Kaoris 3	3.99	9.55	5.08	0.16	292.9	1.76
La Crouen 1	320.92	10.39	3.42	0.33	312.6	0.07
La Crouen 2	99.37	11.05	13.30	1.48	304.6	0.06

Fig. 3. Ternary diagram (N_2-H_2-CH_4) showing the composition of the majors gases in the collected samples.

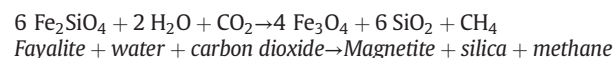Methane generation can also occur with the reaction of carbon-bearing compounds and H_2. In a very general way, H_2 is susceptible to react with any form of carbon in subsurface. $C°$, CO, and CO_2 can react with H_2 as (X being a variable),

$$(2 + X)H_2 + CO_X \rightarrow CH_4 + XH_2O$$

Especially, reaction of dissolved CO_2 with H_2 formed during serpentinization processes can occur. Indeed, if H_2 activity is high enough, it can react with CO_2 according to the classical Sabatier reaction (Sherwood-Lollar et al., 1988, 2006; Abrajano et al., 1988; Szatmari, 1989; Kelley and Früh-Green, 1999; Hosgormez et al., 2008; De Boer et al. 2007; Etiope and Sherwood-Lollar, 2013 and others),

$$4H_2 + CO_2 \rightarrow CH_4 + 2H_2O$$
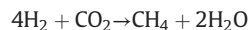
Hence, in this case, methane can be regarded as a by-product of H_2 generation. This reaction is possible at high temperatures (above 200 °C) in totally abiotic conditions (Fischer-Tropsch type reaction; Sherwood-Lollar et al., 1993a; Berndt et al., 1996; McCollom and Seewald, 2001) with catalysis processes (Horita and Berndt, 1999; Foustoukos and Seyfried, 2004), but it is also possible at low temperatures (Sherwood-Lollar et al., 1993b; Etiope et al., 2013) possibly via methanogen microorganisms in hyperalkaline water (Lang et al., 2012; Brazelton et al., 2013). Also H_2 is susceptible to react with organic matter or graphite if H_2-charged fluids migrate through deeply buried sediments, the reaction with graphite being simply,

$$2H_2 + C \rightarrow CH_4$$

For the N_2-H_2-CH_4-rich gas, the $\delta^{13}C$ values of methane are ranging between -34.9 and $-32.4‰$. For the N_2-rich gas, the $\delta^{13}C$ of methane shown values of -39.5 and $-39‰$ in La Crouen but much heavier values in the Roc Aiguille (-16.4 and $-12.1‰$). From these variable values it seems difficult to invoke a unique source of carbon for the methane. The methane with $\delta^{13}C$ values between -40 and $-32‰$ might be simply of thermogenic origin, i.e. issued from thermal cracking of organic matter inside sediments buried below the ophiolitic nappe or simply from the reaction between organic matter and H_2. The total absence of C2+ in the gas associated with this range of $\delta^{13}C$ of CH_4 would rather suggest an origin from a reaction of H_2 with organic matter or graphite present in the sediments below the peridotite nappe. For the methane in the Roc Aiguille, it seems that the heavy $\delta^{13}C$ of CH_4 values are more in agreement with an origin from dissolved inorganic carbon via bacterial processes (Stahl, 1977). Indeed, part of the methane that is found associated with hydrogen could be of parallel generation due to the reduction of dissolved inorganic carbon which may be simply atmospheric CO_2 dissolved in sea water (this vent being located offshore). However, a methanotrophic alteration may also result in heavier $\delta^{13}C$ of residual methane (Aloisi et al., 2002).

As mentioned in the introduction and as discussed above, serpentinization processes can generate H_2 and if any form of carbon is available in this context, it might be the source of the methane found in the gas samples. But what about the origin of nitrogen in the collected samples? Several potential sources can be considered: either deep sources of nitrogen from the mantle or the continental crust, deeply buried sediments (from interstitial water or ammonium in the interspaces of clays), or simply aquifers previously equilibrated with atmosphere (Air Saturated Water, ASW).

6.3. Mixing processes with nitrogen

For the N_2-H_2-CH_4-rich gas, as well as for the N_2-rich gas, noble gases and major gas compounds (H_2, N_2, CH_4) have been used in "mixing diagrams", i.e. figures correlating two chemical ratios with the same denominator. Noble gases being chemically inert,

they are good tracers of transport physical processes and/or interactions between the different phases (e.g. gas and water; Marty and Jambon, 1987; Ballentine et al., 1991, 2002; Battani et al., 2000; Prinzhofer and Battani, 2003; Zhou et al., 2005; Prinzhofer, 2013). In this case, considering any physical fractionation as a process of secondary order, a mixing between two end-members should plot on a straight line (Prinzhofer and Pernaton, 1997) whereas a fractionation trend should give a curved line. It allows characterizing the various possible sources for the gas species, including nitrogen (see for example Jenden et al., 1988). We use in Fig. 4 the two isotopes ^{20}Ne and ^{36}Ar, which are almost entirely coming from the atmosphere (Air), or from aquifers previously equilibrated with atmosphere (ASW), when concentration ratios are used (absolute gas concentrations cannot be compared with water concentrations). This study shows that the $N_2/^{36}Ar$ ratio is variable and always higher than the same ratio for the air or ASW (Fig. 4A), meaning that we cannot simply consider that N_2 is coming directly from the atmosphere or from ASW. Plotting this ratio versus the reciprocal of the ^{36}Ar concentration, two straight lines may be defined for the two gas seep families, each of these straight lines passing through the Air endmember. A mixing model between the air and deep N_2-enriched gas indicates, by fitting the correlation lines, a N_2 content around 98% for the N_2-rich gas family and 53% for the N_2-H_2-CH_4-rich gas family.

The same calculation done with H_2 presents a similar linear trend, and it is possible to calculate H_2 content of 36% for the N_2-H_2-CH_4-rich gas family and 0% for the N_2-rich gas family (Fig. 4B).

Using ^{20}Ne, the same trends are obtained, leading to the same conclusions (Fig. 4C and D), with a small shift for the initial $H_2/^{20}Ne$, possibly due to post-genetic fractionation.

It is also possible to compare the different major gas species (H_2, N_2, CH_4 and He) in the same kind of mixing diagrams, normalizing each of these gases to ^{36}Ar for example (Fig. 5A to D). In these diagrams, as we deal with concentration ratios, it is possible to add the values of the ratios corresponding to ASW, which was not possible using only concentrations. With these plots, it is possible to confirm the gas composition of 36% of H_2 and 53% of N_2 (Fig. 5A), with 15% of associated CH_4 for the N_2-H_2-CH_4-rich family (Fig. 5B). It is also possible to compute a concentration of 5 ppmv of helium for the N_2-H_2-CH_4-rich family, i.e. the atmospheric concentration, without any extra radiogenic helium. Some of the gases present helium concentrations slightly lower than the atmosphere (Carénage 2 and Kaori). This may be explained by the fact that the atmospheric helium, dissolved in water and transferred afterward in the N_2-H_2-CH_4 gas phase may present lower concentrations due to this double process. The N_2-rich gas family presents a concentration of helium around 300 ppmv, confirming that its origin is linked with the deep metasediments and not with the peridotites of the ophiolite (Fig. 5C). ^4He being mainly a radiogenic product derived from the continental crust, it cannot be significantly produced by the mantle rocks of the peridotite nappe. Conversely, we do not observe high $^{40}Ar/^{36}Ar$ ratios in the gas, (close to air composition considering the analytical precision, with six values slightly above and one value slightly below the atmospheric ratio), meaning that the source would be more likely in continental rocks (necessarily below the peridotite nappe) but these rocks should not have been buried enough to release high ^{40}Ar contents (Elliot et al., 1993) but only ^4He. Radiogenic ^{40}Ar (expressed generally as $^{40}Ar* = ^{40}Ar-295.5\ ^{36}Ar$) is indeed relatively low in these samples (< 473 ppmv). It should be noted that Fig. 5C is presented in logarithmic scales, as the whole variation of the ratios would not be readable in linear scales. An excellent correlation between He and H_2 (Fig. 5D) indicates that hydrogen is also linked with a deep source.

The Fig. 6 presents the same principle than Fig. 5A, but using ^{84}Kr instead of ^{36}Ar. ^{84}Kr is also a fossil isotope associated with the air or ASW, but its larger fractionation during its dissolution in water allows to better assess the other endmembers, air or ASW. It appears that the best fit
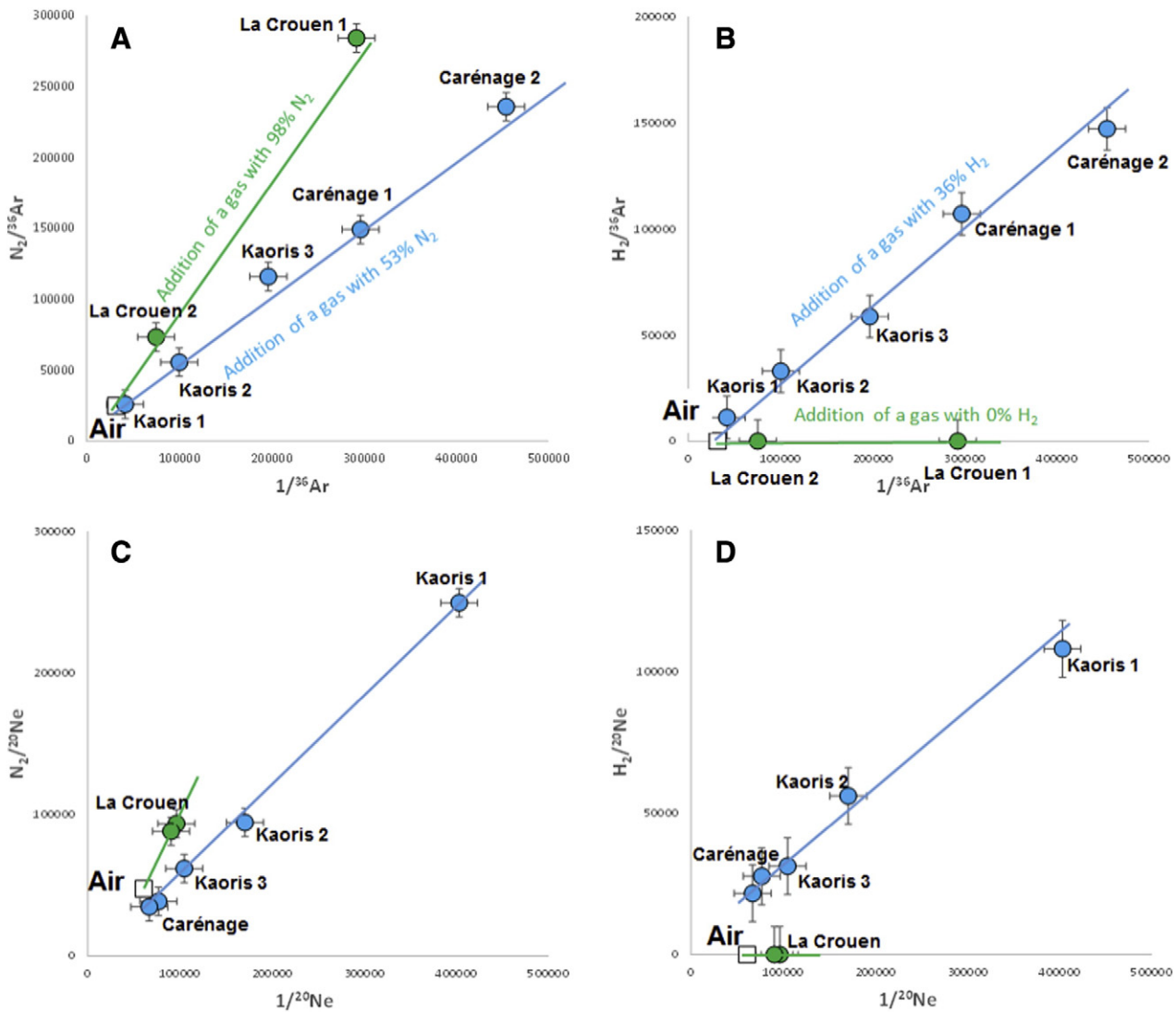
Fig. 4. Mixing diagrams showing the relationships between N_2 and H_2 normalized versus ^{36}Ar and ^{20}Ne contents versus the reciprocals of the ^{36}Ar and ^{20}Ne concentrations.

for a mixing trend is obtained with ASW as one of the endmember. Combining the results of Figs. 5 and 6, this indicates that the two gas families are mixtures between ASW and two different deep gases: one is enriched in H_2, N_2 and CH_4 (36%, 53% and 15% respectively), without any radiogenic helium, whereas another one is enriched in N_2 and radiogenic He (98% and 300 ppmv respectively).

Considering the N_2-H_2-CH_4 family, the analytical data are actually all compatible with a simple mixing between three end-members (1) an atmospheric or ASW end-member, (2) a N_2 and ^4He-rich pole and (3) a H_2, N_2 and CH_4-rich pole without any radiogenic helium. If it is indeed the case, the first end-member (N_2 and ^4He-rich) might find its origin in the continental crust (notably in deeply buried sediments). The occurrence of N_2 associated with ^4He is indeed quite common in continental environments (Sherwood-Lollar et al., 1988; Ballentine and Sherwood Lollar, 2002). In this case, N_2 would probably be issued from the thermal decay of organic matter and/or from ammonium within clay interspaces. The variable concentrations in ^4He between the gas of Prony and the gas of La Crouen might be due to the fact that La Crouen is located in the area where the continental crust is the thickest in New Caledonia, whereas continental material is much thinner in the area of Prony and so less prone to generate ^4He.

Following the same principle of mixing diagrams with the same denominators, Fig. 7A presents the ratios $N_2/^4He$ versus the isotopic ratios of helium $R = {}^3He/^4He$, normalized to the atmospheric air ratio Ra. The

R/Ra ratios are varying between low values, characteristic of radiogenic ^4He addition, and values above unity indicating the presence of mantle helium (with an upper mantle having R/Ra around 8). It appears that the data from both gas series present a clear trend which is not following a straight line. This implies that a process different from simple mixing has to be found in order to explain the data. We suggest the following process in order to fit the correlation (yellow line on Fig. 7A, and model scheme on Fig. 7B): a gas source is composed of air (78% of N_2, 5.15 ppmv of helium) slightly contaminated with mantle helium, giving an initial R/Ra above the air composition at 1.8. An extra amount of nitrogen and helium is added dynamically to this fluid, with a degassing of a deep nitrogen source as presented on Fig. 7C, whereas a ^4He production linked to natural radioactivity gives a linear production through time.

We calculate the helium concentration versus time as:

$$He = He_{air} + \alpha\, t$$

With $He_{air} = 5.15$, α a constant in time^{-1} units (here 20) and:

$$N_2 = N_{2air} + N_{2deep}(1 - \exp(-\beta\, t))$$

With $N_{2air} = 78$, N_{2deep} as the maximum amount of N_2 from a deep source (here 100) and β a constant in time^{-1} units (here 3).
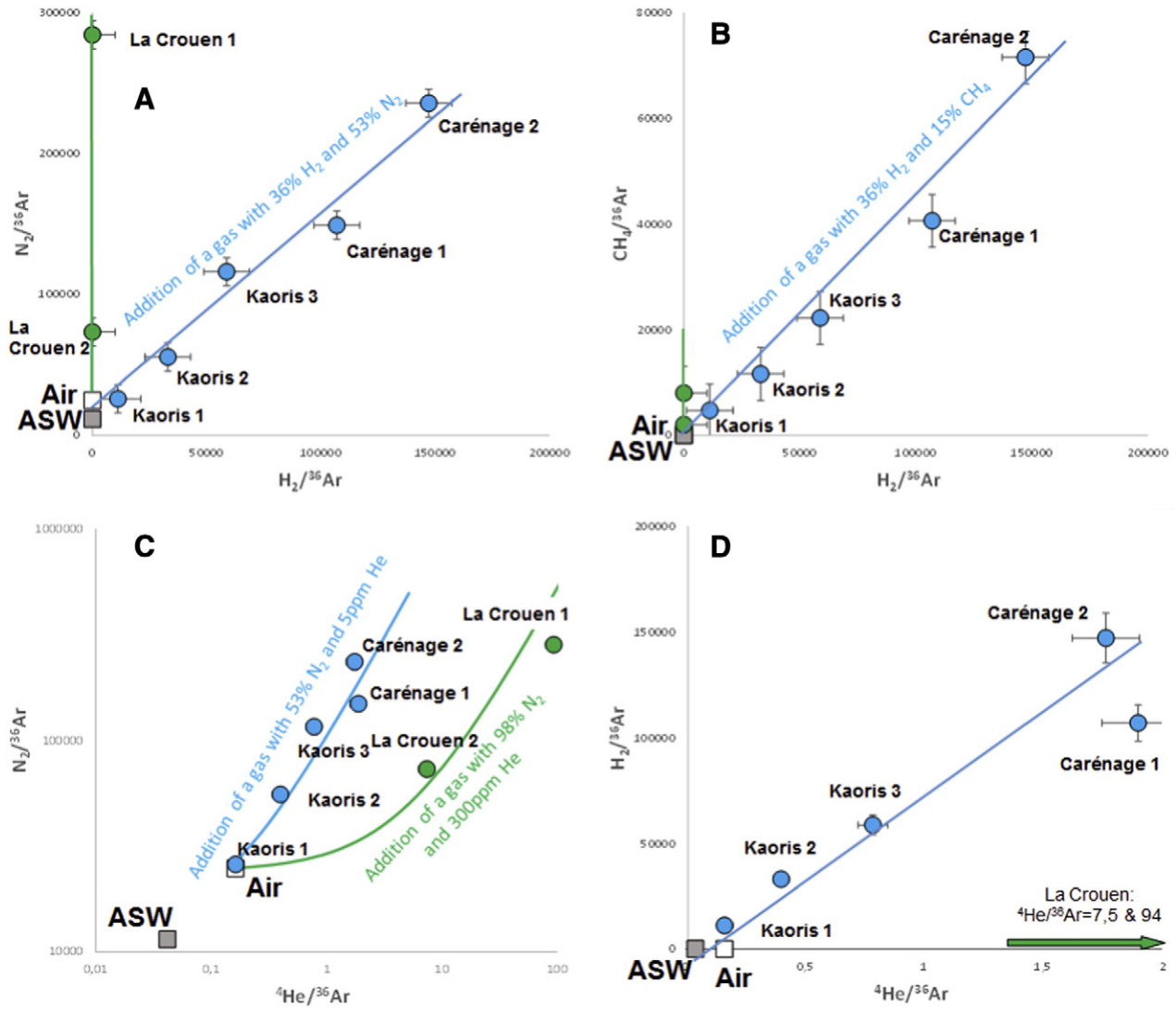
Fig. 5. correlations between the major gas (H_2, N_2, CH_4) and He, normalized to ^{36}Ar.
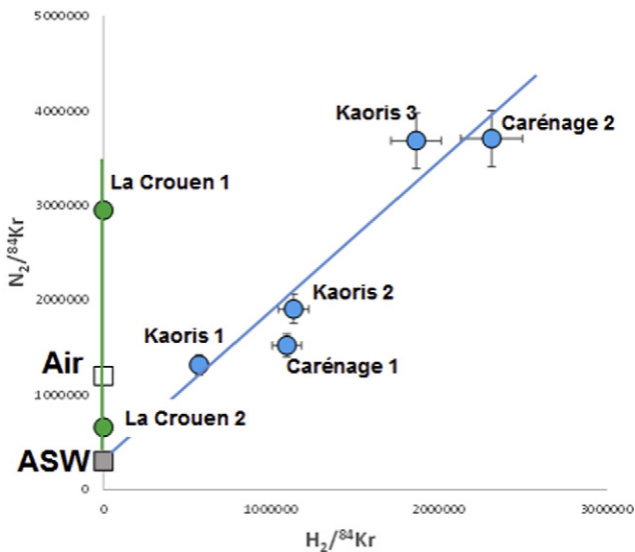

Fig. 6. Correlation between N_2 and H_2 concentrations normalized to the fossil noble gas isotope ^{84}Kr.

Fig. 7A presents the absolute amounts (with a factor 10^4 between N_2 and He) versus time, taken here arbitrary.

The calculation using the ratios N_2/He and R/Ra fits quite well the analytical data, indicating a longer residence time for the N_2-rich gas family than for the N_2-H_2-CH_4-rich one.

Focusing on the two main fossil isotopes ^{20}Ne and ^{36}Ar, whose only reservoirs are the atmosphere and ASW, the data obtained show clearly that an important physical fractionation occurred (Fig. 8): these two isotopes, which are expected to be generally positively correlated (as their main source is air and ASW, and will be more or less diluted in a newly generated gas phase), present a clear inverse correlation, with the air signature far away from the observed correlation. One gas sample of La Crouen is slightly shifted from the inverse correlation, and may be interpreted as contaminated by air during its sampling. In order to interpret the series of gases, a mixing model between two virtual endmembers cannot be an explanation, as a straight line would be expected, which is clearly not the case. We suggest a fractionation model, linked to the dynamic exsolution of neon and argon out of ASW into the sampled gas bubbles. As neon is a lighter molecule, less soluble and diffusing faster than argon, its degassing from the water into a gas phase is more efficient than the degassing of argon. If one considers a finite reservoir of ASW, Fig. 8B represents versus time the degassing of each compound ^{20}Ne and ^{36}Ar. We consider that exsolution of the two compounds ^{20}Ne and ^{36}Ar occur with a different delay due to
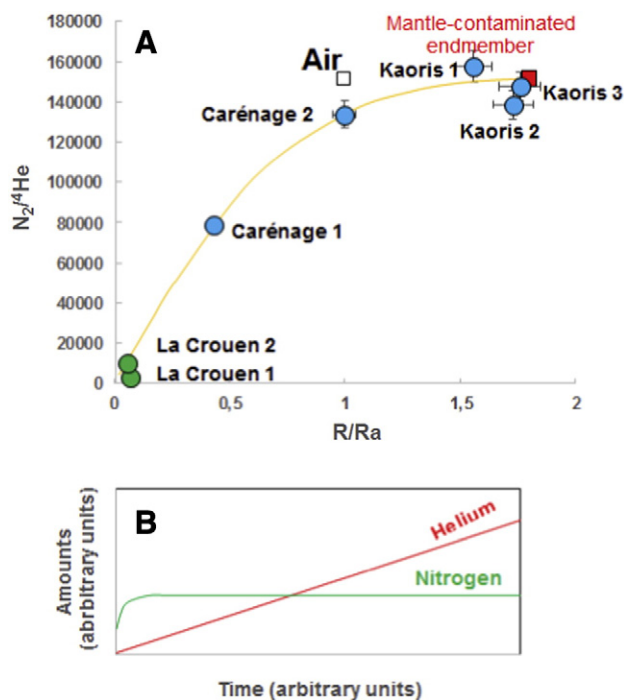
Fig. 7. Correlation between the ratios $N_2/^4He$ versus the helium isotopic ratios $^3He/^4He$ normalized to the atmospheric ratio Ra = 1.4 e-6. A: correlation in linear scales. B: model of generation and degassing of these two gas compounds versus time (arbitrary unit), fitting A and B (yellow lines).

the higher mobility of ^{20}Ne. We model the degassing of a finite amount of water through a simple "bell-curved" evolution with time, assuming a simple water degassing. The used formula is,

$$X = X_{air}exp^{(-(\alpha(t-t_a)^2)}$$
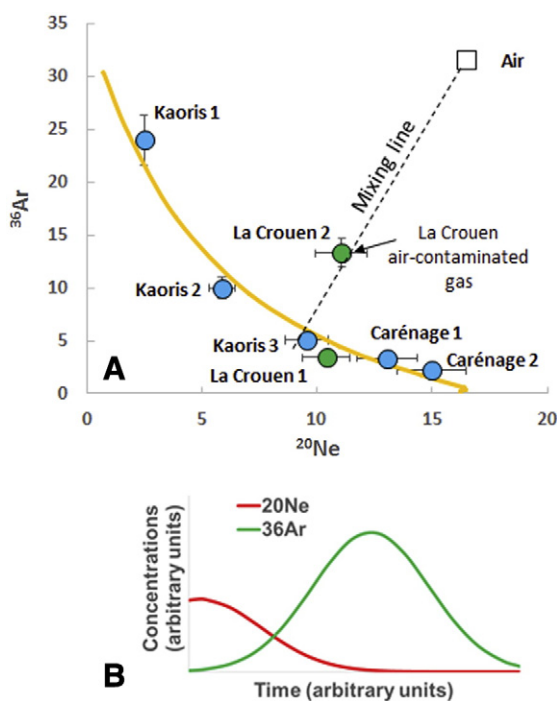
Fig. 8. Inverse correlation between the concentrations of the two main fossil noble gas isotopes ^{20}Ne and ^{36}Ar (A) and model of a confined aquifer degassing progressively (B), fitting the data of A.

where X represents either ^{20}Ne or ^{36}Ar, α a constant, and t_a the time delay for the exsolution.

The values selected for fitting the points of Fig. 8A are a = 0.009 and a = 0.01 for ^{20}Ne and ^{36}Ar respectively. t_a are 1.3 and 22 for ^{20}Ne and ^{36}Ar respectively, in arbitrary units as explained above for Fig. 7B.

The result of such a fractionation is calculated and represented on Fig. 8A with the yellow curve: the gas bubbles are initially enriched in ^{20}Ne and depleted in ^{36}Ar. The continuation of the degassing will favor ^{36}Ar concentrations in the bubbles, as its exsolution is slower, whereas ^{20}Ne will begin to be depleted in the source. This model fits quite well our data and suggests that the dynamic process of gas bubbling is linked to a small amount of associated water, as the depletion of fossil noble gas isotopes is easily visible in the sampled gas bubbles. This suggests that the flux of deep gas is cross-cutting a relatively shallow aquifer which is isolated from a direct equilibrium with the atmosphere. The simplest explanation for this fractionated noble gas exsolution is to assess that the major gas compounds (H_2 and N_2) give the opportunity for the noble gases dissolved in water to equilibrate with this gas phase, possibly during the gas upwelling to the surface.

7. Conclusion

This work has shown that two types of gas are seeping out in and around the ophiolitic units of New Caledonia. One type is N_2-H_2-CH_4-rich, the other type is N_2-rich. In the first type, H_2 and CH_4 are very probably associated with serpentinization processes at low-temperature by reduction of water related to Fe^{2+} oxidation in a relatively shallow aquifer. During these processes, mineral reactions are generating hydrogen at depth in the ultrabasic rocks, and part of this gas contributes to reduction of different sources of carbon (inorganic and organic) producing methane. In the N_2-rich type, N_2 cannot be related with processes only within the ophiolites and we have shown that it cannot come only from ASW. For the two types of gas (N_2-H_2-CH_4-rich and N_2-rich), geochemical data suggest that N_2 has a common origin and comes from depth and not only from air equilibrated aquifers. We interpret the N_2-H_2-CH_4-rich gas family as a result of a mixing between a N_2-rich deep gas coming from deeply buried sediments and a H_2-CH_4-rich gas associated with serpentinization processes inside the ophiolitic nappe (Fig. 9). In all cases, the direct correlation of N_2 with ^4He shows that N_2 has a crustal origin. We suggest that N_2 was either initially dissolved in interstitial water or derived from ammonium present within deeply buried sediments below the ophiolitic complex. The combined study of major gas compounds and noble gas concentrations and isotopic ratios allows to assess a model involving both mixture between different reservoirs (atmospheric gas compounds dissolved in the shallow aquifers, radiogenic imprint, mantle
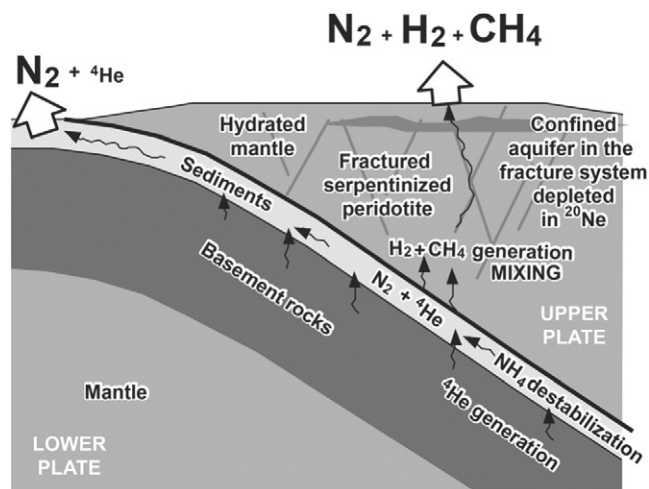

Fig. 9. Conceptual sketch explaining the gas compositions found in New-Caledonia.

contamination) and physical processes fractionating each of these compounds (dynamics of aquifer degassing, continuous generation of radiogenic helium and N_2, etc.). We may conclude that in a first order, the mixing trends are predominant, but that the fractionation processes may be evidenced, quantified and modelled when looking at different noble gas isotopes. Additional studies and notably isotopic studies of nitrogen should give more precise information about its origin.

Appendix A. Supplementary data

Supplementary data to this article can be found online at http://dx.doi.org/10.1016/j.chemgeo.2016.06.011.

References

Abrajano, T.A., Sturchio, N.C., Bohlke, J.K., Lyon, G.L., Poreda, R.J., Stevens, C.M., 1988. Methane–hydrogen gas seeps, Zambales ophiolite, Philippines: deep or shallow origin? Chem. Geol. 71, 211–222.

Abrajano, T.A., Sturchio, N.C., Kennedy, B.M., Lyon, G.L., Muehlenbachs, K., Bohlke, J.K., 1990. Geochemistry of reduced gas related to serpentinization of the Zambales ophiolite, Philippines. Appl. Geochem. 5, 625–630.

Aloisi, G., Bouloubassi, I., Heijs, S.K., Pancost, R.D., Pierre, C., Damsté, J.S.S., Gottschal, J., Forney, L.J., Rouchy, J.-M., 2002. CH_4-consuming microorganisms and the formation of carbonate crusts at cold seeps. Earth Planet. Sci. Lett. 203, 195–203.

Ballentine, C.J., Sherwood Lollar, B., 2002. Regional groundwater focusing of nitrogen and noble gases into the Hugoton-panhandle giant gas field, USA. Geochim. Cosmochim. Acta 66, 2483–2497.

Ballentine, C.J., O'Nions, R.K., Oxburgh, E.R., Horvath, F., Deak, J., 1991. Rare-gas constraints on hydrocarbon accumulation, crustal degassing and groundwater-flow in the Pannonian Basin. Earth Planet. Sci. Lett. 105 (1–3), 229–246.

Ballentine, C.J., Burgess, R., Marty, B., 2002. Tracing fluid origin, transport and interaction in the crust. In: Porcelli, D.R., Ballentine, C.J., Weiler, R. (Eds.), Noble Gases in Geochemistry and Cosmochemistry. Reviews in Mineralogy & Geochemistry Vol. 47, pp. 539–614.

Barnes, I., O'Neil, J.R., Trescases, J.J., 1978. Present day serpentinization in New Caledonia, Oman and Yugoslavia. Geochim. Cosmochim. Acta 42, 144–145.

Battani, A., Sarda, P., Prinzhofer, A., 2000. Geochemical study of Pakistani natural gas accumulations combining major elements and rare gas tracing. Earth Planet. Sci. Lett. 181, 229–249.

Berndt, M.E., Allen, D.E., Seyfried Jr., W.E., 1996. Reduction of CO_2 during serpentinization of olivine at 300 °C and 500 bar. Geology 24, 351–354.

Brazelton, W.J., Morrill, P.L., Szponar, N., Schrenk, M.O., 2013. Bacterial communities associated with subsurface geochemical processes in continental Serpentinite Springs. Appl. Environ. Microbiol. 79 (13), 3906. http://dx.doi.org/10.1128/AEM.00330-13.

Charlou, J.L., Donval, J.P., Fouquet, Y., Jean-Baptiste, P., Holm, N., 2002. Geochemistry of high H_2 and CH_4 vent fluids issuing from ultramafic rocks at the rainbow hydrothermal field (36°14′N, MAR). Chem. Geol. 191, 345–359.

Cipolli, F., Gambardella, B., Marini, L., Ottonello, G., Zuccolini, M.V., 2004. Geochemistry of high-pH waters from serpentinites of the Gruppo di Voltri (Genova, Italy) and reaction path modeling of CO_2 sequestration in serpentinite aquifers. Appl. Geochem. 19, 787–802.

Cluzel, D., Aitchison, J.C., Picard, C., 2001. Tectonic accretion and underplating of mafic terranes in the late Eocene intraoceanic fore-arc of New Caledonia (Southwest Pacific): geodynamic implications. Tectonophysics 340, 23–59.

Cox, M.E., Launay, J., Paris, J.P., 1982. Geochemistry of the low geothermal systems in New Caledonia. Proc. Pacific Geothermal Conference, University of Auckland, New Zealand, Part 2, pp. 453–459.

Deville, E., Prinzhofer, A., Pillot, D., Vacquand, C., Sissman, O., 2010. Peridote-water interaction generating migration pathways of N_2-H_2-CH_4-rich fluids in subduction context: common processes in the ophiolites of Oman, New-Caledonia, Philippines and Turkey. Eos Transactions, American Geophysical Union, Fall Meeting 2010, Abstract# T13 A-2184D.

Elliot, T., Ballentine, C.J., O'Nions, R.K., Ricchiuto, T., 1993. Carbon, helium, neon and argon isotopes in a Po Basin (Northern Italy) natural gas field. Chem. Geol. 106, 429–440.

Etiope, G., Sherwood-Lollar, B., 2013. Abiotic methane on Earth. Rev. Geophys. 51, 276–299 (doi.org/10. 002/rog.20011).

Etiope, G., Vance, S., Christensen, L.E., Marques, J.M., Ribeiro da Costa, I., 2013. Methane in serpentinized ultramafic rocks in mainland Portugal. Mar. Pet. Geol. 45, 12–16.

Foustoukos, D.I., Seyfried Jr., W.E., 2004. Hydrocarbons in hydrothermal fluids: the role of chromium-bearing catalysts. Science 304, 1002–1005.

Horita, J., Berndt, M.E., 1999. Abiogenic methane formation and isotopic fractionation under hydrothermal conditions. Science 285, 1055–1057.

Hosgormez, H., Etiope, G., Yalçın, M.N., 2008. New evidence for a mixed inorganic and organic origin of the Olympic chimaera fire (Turkey): a large onshore seepage of abiogenic gas. Geofluids 8, 263–275.

Jenden, P.D., Kaplan, I.R., Poreda, R.J., Craig, H., 1988. Origin of nitrogen-rich natural gases in the California Great Valley: evidence from helium, carbon and nitrogen isotope ratios. Geochim. Cosmochim. Acta 52, 851–861.

Kelley, D.S., Früh-Green, G.L., 1999. Abiogenic methane in deep-seated mid-ocean ridge environments: insights from stable isotope analyses. J. Geophys. Res. 104 (B5), 10439–10460. http://dx.doi.org/10.1029/1999JB900058.

Kelley, D.S., Karson, J.A., Fruh, G.L., Yoerger, D.R., Shank, T.M., Butterfield, D.A., Hayes, J.M., Schrenk, M.O., Olson, E.J., Proskurowski, G., Jakuba, M., Bradley, A., Larson, B., Ludwig, K., Glickson, D., Buckman, K., Bradley, A.S., Brazelton, W.J., Roe, K., Bernasconi, S.M., Elend, M.J., Lilley, M.D., Baross, J.A., Summons, R.E., Sylva, S.P., 2005. A serpentinite-hosted ecosystem: the Lost City hydrothermal field. Science 307, 1428–1434.

Lang, S.Q., Früh-Green, G.L., Bernasconi, S.M., Lilley, M.D., Proskurowski, G., Méhay, S., Butterfield, D.A., 2012. Microbial utilization of abiogenic carbon and hydrogen in a serpentinite-hosted system. Geochim. Cosmochim. Acta 92, 82–99.

Launay, J., Fontes, J.C., 1985. Les sources thermales de Prony (Nouvelle-Calédonie) et leurs précipités chimiques. Exemple de formation de brucite primaire. Géol. Fr. 1, 83–100.

Marty, B., Jambon, A., 1987. C/^{3}He in volatile fluxes from the solid Earth: implications for carbon geodynamics. Earth Planet. Sci. Lett. 83, 16–26.

McCollom, T.M., Seewald, J.S., 2001. A reassessment of the potential for reduction of dissolved CO_2 to hydrocarbons during serpentinization of olivine. Geochim. Cosmochim. Acta 65, 3769–3778.

Monnin, C., Chavagnac, V., Boulart, C., Ménez, B., Gérard, M., Gérard, E., Quéméneur, M., Erauso, G., Postec, A., Guentas-Dombrowski, L., Payri, C., Pelletier, B., 2014. The low temperature hyperalkaline hydrothermal system of the Prony Bay (New Caledonia). Biogeosci. Discuss. 11, 6221–6267.

Moody, J.B., 1976. Serpentinization: a review. Lithos 9, 125–138.

Neal, C., Stanger, G., 1983. Hydrogen generation from mantle source rocks in Oman. Earth Planet. Sci. Lett. 66, 315–320.

Paris, J.P., 1981. Géologie de la nouvelle-Calédonie. Mem. BRGM 133, 1–278.

Prinzhofer, A., 2013. Noble gases in oil and gas accumulations. In: Burnard, P. (Ed.), The Noble Gases as Geochemical Tracers. Springer, pp. 225–247.

Prinzhofer, A., Pernaton, E., 1997. Isotopically light methane in natural gases: bacterial imprint or segregative migration? Chem. Geol. 142, 193–200.

Prinzhofer, A., Nicolas, A., Cassard, D., Moutte, J., Leblanc, M., Paris, J.P., Rabinovitch, M., 1980. Structures in the New Caledonia peridotites-gabbros; implications for ocanic mantle and crust. Tectonophysics 69, 85–112.

Proskurowski, G., Lilley, M.D., Seewald, J.S., Früh-Green, G.L., Olson, E.O., Lupton, J.E., Sylva, S.P., Kelley, D.S., 2008. Abiogenic hydrocarbon production at lost city hydrothermal field. Science 319 (5863), 604–607.

Sano, Y.A., Urabe, T., Wakita, H., Wushiki, H., 1993. Origin of hydrogen–nitrogen gas seeps. Oman. Appl. Geochem. 8, 1–8.

Sherwood Lollar, B., Lacrampe-Couloume, G., Slater, G.F., Ward, J., Moser, D.P., Gihring, T.M., Lin, L.-H., Onstott, T.C., 2006. Unravelling abiogenic and biogenic sources of methane in the Earth's deep subsurface. Chem. Geol. 226, 328–339.

Sherwood-Lollar, B., Fritz, P., Frape, S.K., Macko, S.A., Weise, S.M., Welhan, J.A., 1988. Methane occurrences in the Canadian shield. Chem. Geol. 71, 223–236.

Sherwood-Lollar, B., Frape, S.K., Fritz, P., Macko, S.A., Welhan, J.A., Blomqvist, R., Lahermo, P.W., 1993a. Evidence for bacterially generated hydrocarbon gas in Canadian shield and Fennoscandian shield rocks. Geochim. Cosmochim. Acta 57, 5073–5085.

Sherwood-Lollar, B., Frape, S.K., Weise, S.M., Fritz, P., Macko, S.A., Welhan, J.A., 1993b. Abiogenic methanogenesis in crystalline rocks. Geochim. Cosmochim. Acta 57, 5087–5097.

Smith, N.J.P., Shepherd, T.J., Styles, M.T., Williams, G.M., 2005. Hydrogen exploration: a review of global hydrogen accumulations and implications for prospective areas in NW Europe. Petroleum Geology Conference Series Vol. 6. Geological Society, London, pp. 349–358.

Stahl, W.J., 1977. Carbon and nitrogen isotopes in hydrocarbon research and exploration. Chem. Geol. 20, 121–149.

Suda, K., Ueno, Y., Yoshizaki, M., Nakamura, H., Kurokawa, K., Nishiyama, E., Yoshino, K., Hongoh, Y., Kawachi, K., Omori, S., Yamada, K., Yoshida, N., Maruyama, S., 2014. Origin of methane in serpentinite-hosted hydrothermal systems: the CH_4–H_2–H_2O hydrogen isotope systematics of the Hakuba Happo hots spring. Earth Planet. Sci. Lett. 386, 112–125.

Szatmari, P., 1989. Petroleum formation by Fischer–Tropsch synthesis in plate tectonics. Am. Assoc. Pet. Geol. Bull. 73, 989–998.

Szponar, N., Brazelton, W.J., Schrenk, M.O., Bower, D.M., Steele, A., Morrill, P.L., 2013. Geochemistry of a continental site of serpentinization, the tablelands ophiolite, Gros Morne National Park: a Mars analogue. Icarus 224, 286–296. http://dx.doi.org/10.1016/j.icarus.2012.07.004.

Vacquand, C., 2011. Genèse et mobilité de l'hydrogène Naturel: source d'énergie Ou Vecteur d'énergie Stockable? (Ph.D thesis) IFPEN-IPGP (174 pages).

Welhan, J.A., Craig, H., 1979. Methane and hydrogen in East Pacific rise hydrothermal fluids. Geophys. Res. Lett. 6, 829–831.

Wood, B.L., 1970. Metamorphosed ultramafites and associated formations near Milford sound, New Zealand. J. Geol. Geophys. 15, 88–128.

Zhou, Z., Ballentine, C.J., Kipfer, R., Schoell, M., Thibodeaux, S., 2005. Noble gas tracing of groundwater/coalbed methane interaction in the San Juan Basin, USA. Geochim. Cosmochim. Acta 69, 5413–5428.